

AD-A043 524

LOCKHEED MISSILES AND SPACE CO INC PALO ALTO CALIF PA--ETC F/G 18/3  
LABORATORY INVESTIGATION OF INFRARED FLUORESCENCE OF CO2, HAES --ETC(U)  
DEC 76 T C JAMES

UNCLASSIFIED

LMSC/D556110

DNA-4238F

DNA001-76-C-0017

NL

1 of 1  
AD  
A043524



END  
DATE  
FILMED  
9-77  
DDC

ADA 043524

9

DNA 4238F

# LABORATORY INVESTIGATION OF INFRARED FLUORESCENCE OF CO<sub>2</sub>

12

HAES Report No. 60

Lockheed Palo Alto Research Laboratory  
3251 Hanover Street  
Palo Alto, California 94304

December 1976

Final Report for Period 1 August 1975—31 December 1976

CONTRACT No. DNA 001-76-C-0017

APPROVED FOR PUBLIC RELEASE;  
DISTRIBUTION UNLIMITED.

DDC  
APPROVED  
AUG 30 1977  
C

THIS WORK SPONSORED BY THE DEFENSE NUCLEAR AGENCY  
UNDER RDT&E RMSS CODE B322076464 S99QAXHI00420 H2590D.

DDC FILE COPY

Prepared for  
Director  
DEFENSE NUCLEAR AGENCY  
Washington, D. C. 20305

UNCLASSIFIED

SECURITY CLASSIFICATION OF THIS PAGE (When Data Entered)

REPORT DOCUMENTATION PAGE		READ INSTRUCTIONS BEFORE COMPLETING FORM
1. REPORT NUMBER DNA 4238F, HAES-60	2. GOVT ACCESSION NO.	3. RECIPIENT'S CATALOG NUMBER
4. TITLE (and Subtitle) LABORATORY INVESTIGATION OF INFRARED FLUORESCENCE OF CO <sub>2</sub> , HAES Report No. 60.	5. TYPE OF REPORT & PERIOD COVERED Final Report for Period 1 Aug 75-31 Dec 76	6. PERFORMING ORG. REPORT NUMBER LMSC/D556110
7. AUTHOR(s) T. C./James	8. CONTRACT OR GRANT NUMBER(s) DNA 001-76-C-0017	
9. PERFORMING ORGANIZATION NAME AND ADDRESS Lockheed Palo Alto Research Laboratory 3251 Hanover Street Palo Alto, California 94304	10. PROGRAM ELEMENT PROJECT, TASK AREA & WORK UNIT NUMBERS NWED Subtask S99QAXHI004-20	
11. CONTROLLING OFFICE NAME AND ADDRESS Director Defense Nuclear Agency Washington, D.C. 20305	12. REPORT DATE December 1976	13. NUMBER OF PAGES 46
14. MONITORING AGENCY NAME & ADDRESS (if different from Controlling Office) 43p.	15. SECURITY CLASS (of this report) UNCLASSIFIED	15a. DECLASSIFICATION DOWNGRADING SCHEDULE
16. DISTRIBUTION STATEMENT (of this Report) Approved for public release; distribution unlimited.		
17. DISTRIBUTION STATEMENT (of the abstract entered in Block 20, if different from Report)		
18. SUPPLEMENTARY NOTES This work sponsored by the Defense Nuclear Agency under RDT&E RMSS Code B322076464 S99QAXHI00420 H2590D.		
19. KEY WORDS (Continue on reverse side if necessary and identify by block number) Infrared Fluorescence 4.3 μm Infrared Bands CO <sub>2</sub> Emission Bands		
20. ABSTRACT (Continue on reverse side if necessary and identify by block number) This report summarizes experiments in which 4.3 μm emission is produced when CO <sub>2</sub> is irradiated with 2.7 μm radiation. Measurements of the attenuation of this signal by various CO <sub>2</sub> filled absorption cells are discussed. Absolute intensity measurements are also discussed. The evidence seems to suggest a large component of the 4.3 μm radiation is due to the bands 021-020 and 101-100. Complete characterization of the composition of the 4.3 μm emission will require detailed radiative transport calculations.		

DDC  
APPROVED  
AUG 30 1977  
MILITARY  
C

DD FORM 1 JAN 73 1473

EDITION OF 1 NOV 65 IS OBSOLETE

UNCLASSIFIED

SECURITY CLASSIFICATION OF THIS PAGE (When Data Entered)

210118

LB

UNCLASSIFIED

SECURITY CLASSIFICATION OF THIS PAGE(When Data Entered)



UNCLASSIFIED

SECURITY CLASSIFICATION OF THIS PAGE(When Data Entered)

ACCESSION for	Wire Section	<input type="checkbox"/>
NTIS	Buff Section	<input type="checkbox"/>
DDC		<input type="checkbox"/>
UNANNOUNCED		
U.S. I. & O. DIV.		
DISTRIBUTION/AVAILABILITY NOTES		
A		

SUMMARY

The High Altitude Effects Simulation (HAES) Program sponsored by the Defense Nuclear Agency since the early 1970 time period, comprises several groupings of separate, but interrelated technical activities, e.g., ICECAP (Infrared Chemistry Experiments - Coordinated Auroral Program). Each of the latter have the common objective of providing information ascertained as essential for the development and validation of predictive computer codes designed for use with high priority DoD radar, communications, and optical defensive systems.

Since the inception of the HAES Program, significant achievements and results have been described in reports published by DNA, participating service laboratories, and supportive organizations. In order to provide greater visibility for such information and enhance its timely applications, significant reports published since early calendar 1974 shall be identified with an assigned HAES serial number and the appropriate activity acronym (e.g., ICECAP) as part of the report title. A complete and current bibliography of all HAES reports issued prior to and subsequent to HAES Report No. 1, dated 5 February 1974 entitled, "Rocket Launch of an SWIR Spectrometer into an Aurora (ICECAP 72)," AFCRL Environmental Research Paper No. 466, is maintained and available on request from DASIAC, DoD Nuclear Information and Analysis Center, 816 State Street, Santa Barbara, California 93102, Telephone (805) 965-0551.

This report, which is the final report under DNA Contract DNA001-76-C-0017 is the 60th report in the HAES series, and covers the technical activities performed during the period 1 Aug. 1976 through 31 December 1976. The purpose of the work described herein was to investigate the fluorescence of CO<sub>2</sub> at 4.3 microns when irradiated with radiation near 2.7 microns, and to determine the intensity and composition of the resulting fluorescent radiation and the mechanisms responsible for producing the observed spectral characteristics of this radiation.

705622

## PREFACE

The author would like to thank Dr. J. B. Kumer for advice and discussions which have been crucial in leading to a successful observation of  $4.3 \mu\text{m}$  emission and which have led to an understanding of the problems involved in fully understanding the experimental results. Calculations of the Band Transmission and Equivalent widths were carried out using computer programs developed by Dr. Kumer. Discussions with Dr. A. Roche have been useful in carrying out the calibration measurements.

## TABLE OF CONTENTS

I.	Introduction	5
II.	Calculation of Linewidths, Cross Section and the Band Transport Functions W and T	10
	II-1 Definition and Formulas	10
	II-2 Numerical Magnitudes	14
III.	Calibration of Detector	15
IV.	Calculation of Expected Signals	18
V.	Attenuation of the 4.3 $\mu\text{m}$ Signal by Various $\text{CO}_2$ Filter Cells	21
VI.	Determination of Approximate Quenching Rates From Absolute Intensity Measurements	31
VII.	Summary and Discussion of Results	39
	References	42

## I. INTRODUCTION

This report describes experimental measurements of fluorescence of  $\text{CO}_2$  at  $4.3 \mu\text{m}$  when irradiated with radiation at  $2.7 \mu\text{m}$ . The discussion of this section can be more clearly followed by reference to the partial energy level diagram in figure 1.

$\text{CO}_2$  has two combination bands of moderate intensity which occur near  $2.7 \mu\text{m}$ . These are the  $02^{\circ}1 - 000$  band which is centered at  $2.77 \mu\text{m}$  and the  $101-000$  band centered at  $2.69 \mu\text{m}$ . Excitation of molecules in these bands produces excited molecules which are able to radiatively decay via several routes.

For the isolated molecules, that is completely in the absence of collisions, the predominant radiative decay mechanism in the emission of radiation centered near  $4.3 \mu\text{m}$  which corresponds to transitions in which  $\nu_3$  is decreased by unity. A simple calculation (see James and Kumer (1) ) indicates that the transition  $02^{\circ}1 \rightarrow 02^{\circ}0$  and  $101 \rightarrow 100$  which result in fluorescence at  $4.3 \mu\text{m}$  should occur with a 95% probability. The re-emission of  $2.77$  and  $2.69 \mu\text{m}$  bands occurs with approximately a 5% probability.

Additional possibilities for radiative decay include the bands  $02^{\circ}1-011$  and  $101-011$  at  $16.4 \mu\text{m}$  and  $14.1 \mu\text{m}$  respectively, the bands  $02^{\circ}1 \rightarrow 20^{\circ}0$  and  $101 \rightarrow 200$  at  $12.25 \mu\text{m}$  and  $10.9 \mu\text{m}$  respectively, and the bands  $02^{\circ}1-12^{\circ}0$  and  $101 \rightarrow 12^{\circ}0$  at  $10.62 \mu\text{m}$  and  $9.58 \mu\text{m}$  respectively. All of these bands together account for less than one percent of the total radiative decay and may be disregarded in calculating the efficiency of  $2.7 \mu\text{m}$  radiation in producing  $4.3 \mu\text{m}$  radiation.

In order to observe this fluorescence in the laboratory it is necessary to conduct measurements at sufficiently low pressures that quenching and energy transfer processes do not reduce the population of the levels  $101$  and  $02^{\circ}1$  at a rate which is so rapid as to completely quench the  $4.3 \mu\text{m}$ .

In a laboratory measurement of fluorescence at  $4.3 \mu\text{m}$  produced by  $2.7 \mu\text{m}$



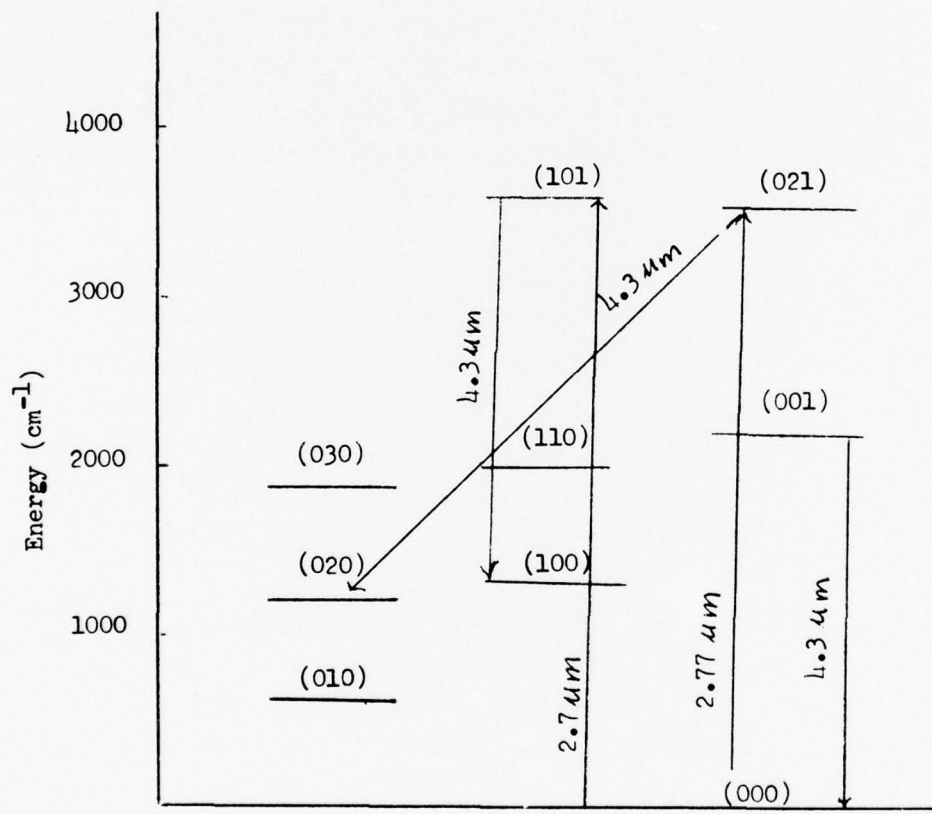
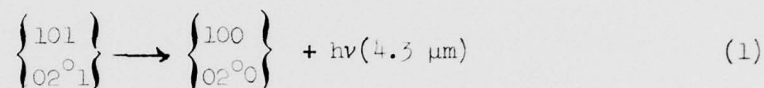


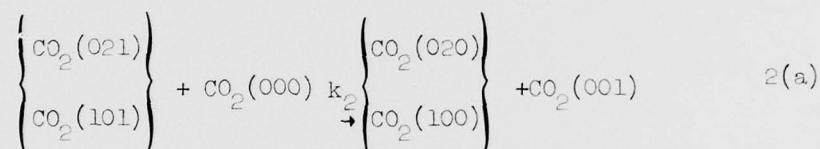
Figure 1 Partial Energy Level Diagram for CO<sub>2</sub>

excitation, there are several possible transitions which can contribute to fluorescence at 4.3  $\mu\text{m}$ . These possibilities are summarized here.

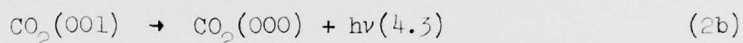
At low pressures where radiation is rapid compared with energy transfer and quenching collisions, the main component of 4.3  $\mu\text{m}$  radiation will be due to the bands



At moderate pressures of pure  $\text{CO}_2$  one expects that the main mechanism for production of radiation would be due to the following sequence of events:



Followed by



Whether or not emissions (1) or 2(b) is predominant depends on the pressures used and on the rate constant  $k_2$  for the energy transfer 2(a).

When this work was originally proposed we were not sure how large  $k_2$  might be, but recognized that it might be as rapid or possibly even more rapid than the transfer reaction



The rate constant for this reaction is  $5.2 \times 10^{-13}$ . A transfer rate this rapid for the corresponding reactions 2(a) would indicate that pressures in the range of 125 microns Hg would produce molecules in the 001 level at a rate more than five times as fast as the radiative decay in Eqn. (1). The possibility was therefore raised that most of any 4.3  $\mu\text{m}$  radiation produced would be from resonance radiation  $001 \rightarrow 000$  rather than the fluorescence due

to 101 → 100 and 021 → 020.

These considerations suggested that reactions 2(a) would require working at low pressures with a corresponding decrease in overall signal at 4.3 which is limited by the amount of 2.7 μm radiation absorbed.

In a summary by Nickerson<sup>(2)</sup> of rate constants for CO<sub>2</sub>, the rate constant quoted for reactions 2(a) was nearly an order of magnitude larger than the corresponding reaction 3 for N<sub>2</sub>. The quoted rate constant was approximately  $7 \times 10^{-14}$ . This would suggest that process 2 would not greatly interfere with our measurements.

Originally we expected that we could distinguish between fluorescence bands 101 → 100 and 021 - 020 and the resonance band 001 → 000 by inserting a CO<sub>2</sub> cell between the fluorescence cell and the detector. This should absorb any resonance radiation and transmit the fluorescence bands: as will be discussed further in this report, this may not be as simple as we had thought.

Our initial attempts at observing the fluorescence were unsuccessful. We now attribute this failure mainly to the use of an inadequate light source, although results which we have obtained using a Blackbody Source of much greater area suggests that our earlier measurements should have produced some measurable signal.

During the period in which we were having difficulty obtaining results, we became aware of studies by Finzi and Moore<sup>(3)</sup> in which a laser at 2.7 μm was used to excite specific rotational lines in the bands 021-000 and 101-000. Following a pulsed excitation at 2.7 μm, they observed emission of 4.3 μm radiation. From measurements of the rate of decay of this signal they obtained a rate constant for reactions 2(a) of  $1.3 \times 10^{-10}$ . Such a large value for this rate constant suggests that very little fluorescence should be observed in our experiments since at a pressure of 100 μm Hg =  $3.26 \times 10^{15}$ /cc at 296°K, the deactivation of 101 and 021 levels would occur at a rate of  $\sim 4.2 \times 10^5 \text{ sec}^{-1}$  compared with a radiative rate of  $420 \text{ sec}^{-1}$ . Thus most of the 4.3 μm radiation observed would have to come from the 001-000 resonance band.

This rate is in fact so rapid that at pressures of the order of 1 Torr we might expect a large number of  $\Delta v_3 = 1$  bands due to rapid equilibration of  $v_3$  between various  $v_1 v_2$  levels and isotopic  $\text{CO}_2$  molecules which are significantly populated.

In this report we describe attempts which have been made to date to characterize emission at  $4.3 \mu\text{m}$  by means of a  $\text{CO}_2$  filter and by varying the linewidth in emitting and absorbing gases. Our results are not considered to be definitive at the present time.

The bands behave with respect to self-absorption as though they arise from the 101-000 and 021-020 transitions. This is in direct contradiction to what we expect from the laser studies which yield  $k_2 \sim 1.3 \times 10^{-10}$ . If our results are not due to these fluorescent bands then they must contain a large contribution of the 001-000 resonance band. The indications from our experiments are that this is not the case either.

Our report also summarizes some measurements of the absolute intensity of the  $4.3 \mu\text{m}$  emission. These results indicate that the total rate of quenching of levels emitting at  $4.3 \mu\text{m}$  is much smaller than we would expect for the fluorescence bands if the results of Finzi and Moore are correct in that  $k(2_a)$  is of the order of  $1.3 \times 10^{-10}$ . If it is assumed that we are actually observing the resonance band 001-000 and some other hot bands and isotopic bands, then our absolute intensity measurements yield a quenching rate constant which is qualitatively in agreement with existing rate constants for  $\text{CO}_2$ . In this case, however, we fail to see why there is no appreciable self absorption in our observed  $4.3 \mu\text{m}$  emission.

We will return to a brief discussion of this point after presenting a summary of our results.

## II. CALCULATION OF LINEWIDTHS, CROSS SECTIONS, AND THE BAND TRANSPORT FUNCTIONS W AND T

### II-1 Definitions and Formulas

In this section we summarize calculations which are used in the discussion throughout this report. For additional details and examples, the reader is referred to Kumer and James<sup>(4)</sup>.

The integrated absorption for a single line of intensity  $S$  in  $\text{cm}^{-1}$  is given by

$$W = \int (1 - e^{-k(\nu)\ell}) d\nu$$

$W$  is the equivalent width. The quantity  $k(\nu)$  is the absorption coefficient and  $\ell$  the path length.

The total line strength  $S$  is related to  $k(\nu)\ell$  by  $S = \int k(\nu)\ell d\nu$  where the integration is carried out over the entire line profile.

For some purposes it is convenient to introduce a width function which instead of integrating over frequency, integrates over a dimensionless variable  $x$  which is defined as

$$x = \left( \frac{\nu - \nu_0}{\Delta\nu_D} \right)$$

where  $\Delta\nu$  represents the width of a Doppler Shaped line at a point where the intensity is down by a factor of  $1/e$  from the intensity at line center. In this case the width function is dependent on the value of the cross section at line center and the number density of absorbing molecules and is given by

$$W(N\sigma) = \frac{1}{\pi^{1/2}} \int \left( 1 - e^{-N\sigma_0 Q(x)} \right) dx$$

where  $x = \frac{\nu - \nu_0}{\Delta\nu_D}$  and  $Q(x)$  represents the shape of the line. The usual half-width of a Doppler shaped line  $\gamma_D$  is related to  $\Delta\nu_D$  by,

$$\Delta\nu_D = \gamma_D / \sqrt{\ln 2}$$

where

$$\gamma_D = \sqrt{\frac{2kT \ln 2}{m c^2}}$$

For the Doppler Shaped lines, the half-width can be shown to be

$$\gamma_D = 3.58 \times 10^{-7} \sqrt{\frac{T}{M}} \nu (\text{cm}^{-1})$$

The Cross section at line center is given by:

$$\sigma_0 = \frac{4.158 \times 10^{-13}}{\gamma_D (\text{cm}^{-1})} \cdot f$$

The transmission function for a single line determines the amount of radiation in a single line that can be transmitted through a sample for which the optical thickness at line center is  $N\sigma_0$ . This is given by

$$T(N\sigma_0) = \frac{1}{\sqrt{\pi}} \int Q(x) e^{-N\sigma_0 Q(x)} dx$$

In the case of a rotation-vibration band characterized by an f-number for the entire band, the corresponding cross section for a single rotational line is

$$\sigma_{J'', J'} = \sigma_0 S_{J'', J'}^{J''} \quad \text{where}$$

$S_{J'', J'}^{J''}$  is the rotational line strength and is given for  ${}^1\Sigma - {}^1\Sigma$  Transitions by:

$$S_{J'', J'}^{J''} = \begin{cases} \frac{J''}{2J'' + 1} & \text{for R Branch lines} \\ \frac{J'' + 1}{2J'' + 1} & \text{for P Branch lines} \end{cases}$$

The value of  $N\sigma_0$  for a single rotational line is related to the value for an entire rotation-vibration band by

$$N_{J''}\sigma_{J''J'} = (N\sigma_0)_{\text{band}} \cdot X_{J''} S_{J'' \rightarrow J'}$$

where  $X_{J''}$  represents the fraction of molecules in the level  $J''$ . The width function for an entire rotation vibration band is given as

$$W(N\sigma_0) = \sum_{J''J'} W(N_{J''}\sigma_{J''J'})$$

Similarly, the transmission functions for an entire rotation-vibration band is given by

$$T(N\sigma) = \sum_{J''J'} X_{J''} T(N_{J''}\sigma_{J''J'})$$

The calculations which we have summarized here are carried out for Doppler Shaped lines and also for lines having a Voigt profile. In the case of a Voigt profile the function  $Q(x)$  appropriate to a Voigt profile must be used. These calculations will differ depending on the value of a parameter  $a$  which gives the ratio of the pressure broadened width  $\gamma_L$  to the e-fold Doppler width  $\Delta\nu_D$ . The pressure broadened half width is simply given by

$$\gamma_L = \gamma^0 P$$

where  $\gamma^0$  is the width at atmospheric pressure and  $P$  is the pressure.

As a final point we note that the equivalent width and line strength have the same relative magnitudes as the width function  $W(N\sigma)$  and  $N\sigma$ . That is

$$\frac{W(S)}{S} = \frac{W(N\sigma)}{N\sigma}$$

These results are used in calculating  $N\sigma_0$  values required for various pressures

and path lengths described in this report.

Doppler Line width

$$\begin{aligned} \text{For } 4.3 \text{ } \mu\text{m Bands } \gamma_D &= 2.18 \times 10^{-3} \text{ cm}^{-1} \\ \text{021-000 Band } \gamma_D &= 3.35 \times 10^{-3} \text{ cm}^{-1} \\ \text{101-000 Band } \gamma_D &= 3.45 \times 10^{-3} \text{ cm}^{-1} \end{aligned}$$

In the case of pure  $\text{CO}_2$  the pressure broadened width is  $\approx .085 \text{ cm}^{-1}/\text{ATM}$ .  
Therefore at 1 Torr

$$\gamma_L = (.085) \frac{1}{760} = 1.1 \times 10^{-4} \text{ cm}^{-1}$$

In the case of pressure broadening by Ne with an assumed average half-width of  $.05 \text{ cm}^{-1}/\text{ATM}$ , the linewidth due to pressure broadening is

$$\gamma_L = (.05) \frac{1}{760} = 6.5 \times 10^{-5} (\text{cm}^{-1}/\text{Torr Ne})$$

In the case of pure  $\text{CO}_2$  at a pressure of a few Torr, the Doppler linewidth is an order of magnitude greater than the Lorentz pressure broadened halfwidth so that the lines are nearly Doppler in shape.

At approximately 60 Torr of Ne, the lines in bands near  $4.3 \text{ } \mu\text{m}$  have a Voigt profile with a value of  $a = \gamma_L/\Delta\nu_D \approx 1.5$ . The bands near  $2.7 \text{ } \mu\text{m}$  will have a value of  $\gamma_L/\Delta\nu_D \approx 1$ .

In cases where we have calculated band function W and T, the calculations have been carried out to  $J = 100$ .

In addition to the Bands for which we list  $N_0$  values, we have also carried out calculations for a number of isotopic bands. The corresponding  $N_0$  values are obtained by multiplying the above  $N_0$  values by the isotopic abundance ratios. For the isotopic 636, 628, and 627 the abundances are:  $1.1 \times 10^{-2}$ ,  $4.06 \times 10^{-3}$ , and  $7.3 \times 10^{-4}$ . The notation 636 means  $^{16}_0 \text{ }^{13}_C \text{ }^{16}_0$  etc.



## II-2 Numerical Magnitudes

At a temperature of 296° C the number density at a pressure of 1 Torr is given by

$$\begin{aligned} &= (2.69 \times 10^{19}) \left( \frac{273}{296} \right) \left( \frac{1}{760} \right) \\ &= 3.26 \times 10^{16} / \text{cm}^3 \end{aligned}$$

f-numbers for bands of interest are

101-000	f = 1.97 x 10 <sup>-6</sup>
021-000	f = 1.57 x 10 <sup>-6</sup>
001-000	f = 1.14 x 10 <sup>-4</sup>

For other bands involving  $\Delta v_3 = 1$ , the f number is taken to be  $1.14 \times 10^{-4}$ .

The population of the levels 020 and 100 which are the ground state of the 021-020 and 101-100 fluorescent bands are

$$\begin{aligned} N(020) &= N(000) \times 1.9 \times 10^{-3} \\ N(100) &= N(000) \times 1.5 \times 10^{-3} \\ N(010) &= N(000) \times 7.7 \times 10^{-2} \end{aligned}$$

This results in the following values of  $N\sigma_0$  for Doppler Shaped lines at a pressure of 1 Torr and a pathlength of 1 cm.

Band	$N\sigma_0$ (1 cm path, 1 Torr pressure)
021-000	6.32
101-000	7.73
001-000	707.4
021-020	1.344
101-100	.813
011-010	54.74

### III. Calibration of Detector

The InSb detector used in the measurements is calibrated using a blackbody source displaced at a distance of 25 cm from the detector. The same 4.3  $\mu\text{m}$  filter as used in measurements of the radiation from the  $\text{CO}_2$  fluorescence signal is used in making this calibration. This filter is shown in fig. (2).

Given a blackbody source with aperture  $A_S$  and a blackbody radiance of  $\frac{W_\lambda}{\pi}$ , the total amount of radiation striking a detector of area  $A_D$  at a distance  $d$  away is given by

$$\text{Signal} = \int \left( \frac{W_\lambda}{\pi} \right) \frac{A_S A_D}{d^2} R_\lambda f_\lambda d\lambda$$

In this expression  $R_\lambda$  is the responsivity of the detector in units of mv/watt and  $f_\lambda$  is a function describing the transmission of the detector window and/or any filters which are placed in front of the detector.

In our experiments we use the filter at 4.3  $\mu\text{m}$  shown in figure (2) which has a bandwidth of 0.271  $\mu\text{m}$  and a peak transmission of approximately 70%. The response of the detector is essentially constant over such a small spectral range. Therefore we take  $f_\lambda$  as

$$f_\lambda = (0.271 \mu\text{m}) \times (0.7)$$

and  $W_\lambda$  and  $R_\lambda$  are given the value they have at 4.3  $\mu\text{m}$ .

The source temperature used in these measurements was 1148.4 $^\circ\text{K}$ . The source was an Infrared Industries calibrated Blackbody. Thus  $(w/\pi) = 0.435 \text{ watts/cm}^2\text{-Sr-}\mu\text{m}$ .

The Blackbody Aperture was selected to be 0.025 inches in diameter which gives  $A_S = 3.17 \times 10^{-3} \text{ cm}^2$ . The detector has an area of  $3.14 \times 10^{-2} \text{ cm}^2$ . Putting these numerical quantities into the above expression yields

$$\begin{aligned} \text{Signal (mv)} &= R(\text{mv/watt}) \times (.465) \frac{(3.17 \times 10^{-3})(3.14 \times 10^{-2})}{(25)^2} (.271)(.7) \\ &= R \left( \frac{\text{mv}}{\text{watt}} \right) \times (1.35 \times 10^{-8} \text{ watts}) \end{aligned}$$

It is necessary to make a correction to this figure due to the fact that in a 25 cm path through the laboratory, the 4.3  $\mu\text{m}$  band of  $\text{CO}_2$  will absorb some of the radiation from the blackbody.

The Band strength of  $\text{CO}_2$  is  $2706 \text{ cm}^{-1}/\text{Atm-STP}$ . The mixing ratio of  $\text{CO}_2$  is taken as  $3.2 \times 10^{-4}$  and the path length is 25 cm. Thus the total band strength due to  $\text{CO}_2$  between the detector and the source is

$$\text{Band Intensity} = (2706)(3.2 \times 10^{-4}) \left( \frac{273}{296} \right) (25) = 19.9 \text{ cm}^{-1}$$

For this value of the Band intensity some of the stronger lines are nearly optically thick at line center, having transmission of the order of  $e^{-2.8} \sim 4\%$ . Therefore a more accurate estimate of the amount of absorption is given by the band equivalent width, which will be less than the value of  $19.9 \text{ cm}^{-1}$  given above.

The Band equivalent width has been calculated from the sum of equivalent widths of individual lines in the band. For a single line the width  $W$  is related to the strength  $S\ell$  by

$$W = 2\pi\gamma f(x) \text{ where } x = \frac{S\ell}{2\pi\gamma}$$

The function  $f(x)$  has been tabulated by Kaplan and Eggers<sup>(5)</sup>. Using their table and carrying out the calculation of  $W$  for all lines contributing significantly to the band strength we obtain

$$W_{\text{band}} \approx 15 \text{ cm}^{-1}$$

Now since  $\Delta\lambda(\mu\text{m}) = 10^{-4} \lambda^2 \Delta\nu(\text{cm}^{-1})$ , the band equivalent width in  $\mu\text{m}$  is:

$$W_{\text{band}} \approx 0.027 \mu\text{m}.$$

This result indicates that in the calibration, it is necessary to reduce the value of the filter bandwidth of 0.271 by 0.027  $\mu\text{m}$  which changes the value of  $1.35 \times 10^{-8}$  watts reaching the detector to a value which is smaller by a factor of  $(.271 - .027)/(.271)$ . Therefore we finally obtain

$$S(\text{mv}) = R_{\lambda} (1.21 \times 10^{-8} \text{watts})$$

The average of several measurements of the signal was

$$\text{Signal} \simeq 2.6 \text{ millivolts}$$

From these results we obtain the Responsivity of the detector as

$$R_{\lambda} = (2.6 \text{ mv}) / (1.21 \times 10^{-8} \text{ watts}) =$$

$$R_{(4.3)} = 2.14 \times 10^8 \text{ mv/watt}$$

#### IV. Calculation of the Expected Signals

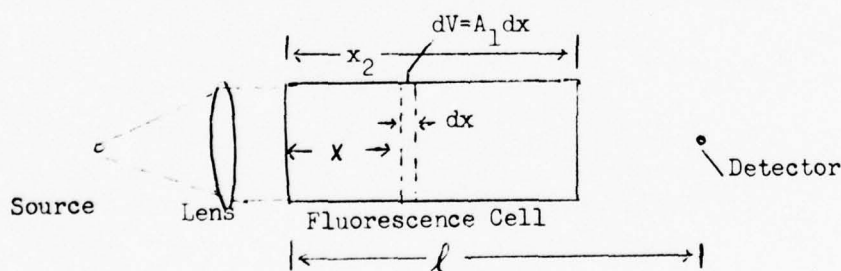
The absorption from a given beam of light can be calculated from the known intensity of the beam and the width function describing the absorption for an entire rotation vibration band.

The width function for a band is the sum of the equivalent widths of individual absorption lines and is given by

$$W_{\text{band}} = \sum_{J', J''} \int \left( 1 - e^{-N_{J''} \sigma_{J', J''} x} \right) dv$$

In the case where all lines are optically thin, then the bandwidth is equal to the total band strength. In the case where many of the lines are saturated, then it is necessary to carry out a detailed calculation. We begin by considering the optically thin case, and later will extend our results to account for cases in which more detailed calculations are required.

Consider the following Geometrical Arrangement.



Given a Blackbody Radiance of  $\frac{W}{\pi}$  watts/cm<sup>2</sup>-Sr- $\mu$ m, it is convenient to express this in watts/cm<sup>2</sup>-Sr-cm<sup>-1</sup>.

For a given solid angle  $\Omega_s$  extended by the lens  $L_1$  as measured from the source, a given area  $A_1$  of the lens  $L_1$  and a given area of the source  $A_s$ , the flux in watts/cm<sup>2</sup> cm<sup>-1</sup> in the sample cell of cross sectional area  $A_1$  is given by

Flux of Incident Radiation

$$F = \left( \frac{W}{\pi} \right) \frac{\Omega_s A_s}{A_1}$$

If  $S_b$  is the band strength (per cm of path) of absorber in the cell, then the amount of radiation absorbed per unit volume is  $F[S_b dx]$ . Within this volume element, an amount of radiation  $[F S_b dx] \cdot R$  will be emitted into  $4\pi$  steradians.  $R$  is the fraction of excited molecules which emit. For a detector of size  $A_D$  this subtends a solid angle  $\Omega_x$  with points in  $dV$ . Therefore the fraction of this radiation striking the detector is given by  $\frac{\Omega_x}{4\pi}$ . For  $l$  and  $x$  as shown in the figure  $\Omega_x$  is just  $\frac{A_D}{(l-x)^2}$ .

Combining these factors results in the following value of radiation striking the detector from a volume element  $A_1 dx$

$$dS = \left( \frac{W}{\pi} \right) \frac{\Omega_s A_s}{A_1} \cdot R A_1 S_b \cdot \frac{\Omega_x}{4\pi} dx$$

which yields a total signal of

$$S = \left( \frac{W}{\pi} \right) \Omega_s A_s S_b R \frac{A_D}{4\pi} \int_0^{x_2} \frac{dx}{(l-x)^2}$$

$$= \left( \frac{W}{\pi} \right) \Omega_s A_s S_b R \frac{A_D}{4\pi} \left[ \frac{1}{(l-x_2)} - \frac{1}{l} \right]$$

In our experiments we have a filter at the exit aperture of the blackbody which only transmits 2.7  $\mu$ m radiation. There is also a filter in front of the detector which only transmits 4.3  $\mu$ m radiation. Therefore this expression

for the signal would also have to be multiplied by the transmission of these filters  $T_{2.7}$  and  $T_{4.3}$ . In the event that the emitting bands are optically thick these will be a further reduction in the signal by an amount  $W(N_0)/N_0$  due to self absorption. Finally an additional factor of  $(2.7)/(4.3)$  is required since photons at  $4.3 \mu\text{m}$  which are emitted are less energetic than  $2.7 \mu\text{m}$  photons by the ratio  $2.7/4.3$ . Since our signal is expressed in watts rather than photons/sec., this correction factor is necessary.

Some additional refinements to this calculation are discussed in section VI when we describe some absolute intensity measurements.

## V. Attenuation of the 4.3 $\mu\text{m}$ Signal by Various $\text{CO}_2$ Filter Cells

We have carried out a number of experiments aimed at characterizing the 4.3 radiation which we have observed following irradiation of  $\text{CO}_2$  by 2.7  $\mu\text{m}$  radiation. Various experimental arrangements have been used and are illustrated in figure (3) arrangements 1-B, 2-B, and 3-B.

Initially we used the arrangement shown in 1-B in which a 16.6  $\mu\text{m}$  fluorescence cell was followed by a cell of 1.8 cm length which was to act as a filter for  $\text{CO}_2$  bands which terminate on the ground state (000) of  $\text{CO}_2$ . A 4.3  $\mu\text{m}$  filter shown in figure (2) was placed in front of the detector.

With this arrangement we observed a signal of  $2.97 \times 10^{-11}$  watts when the 16.6 cm fluorescence cell had 1 Torr of  $\text{CO}_2$  plus 70 Torr of Ne with the 1.8 cm filter cell removed. Evacuation of the fluorescence cell resulted in loss of this signal. Inserting the filter cell which was filled with 8 Torr  $\text{CO}_2$  and 60 Torr Ne did not reduce the observed signal, in fact it appeared that there may have been a slight increase in signal, of the order of 2%, which may be due to some fluorescence occurring in the filter cell since there was no filter between the fluorescence cell and the filter cell to block out 2.7  $\mu\text{m}$  radiation.

Although several different choices of pressures were utilized with this arrangement, we consider this data to be unsatisfactory because of the possible complication of both fluorescence and absorption occurring in the  $\text{CO}_2$  filter cell. To eliminate this complication we placed the 4.3  $\mu\text{m}$  filter between the fluorescence cell and the filter cell as shown in arrangement 2-B of figure 3.

Using arrangement 2-B and the filter cell the same as before (8 Torr  $\text{CO}_2$  + 60 Torr Ne) and the fluorescence cell filled with 1 Torr of  $\text{CO}_2$  + 60 Torr Ne a signal  $1.2 \times 10^{-11}$  watts was observed. (The smaller signal in this arrangement is due to the smaller aperture of the filter cell when the 4.3  $\mu\text{m}$  filter is placed at the window of the filter cell.) Again, the signal was unchanged by inserting or removing the filter cell.



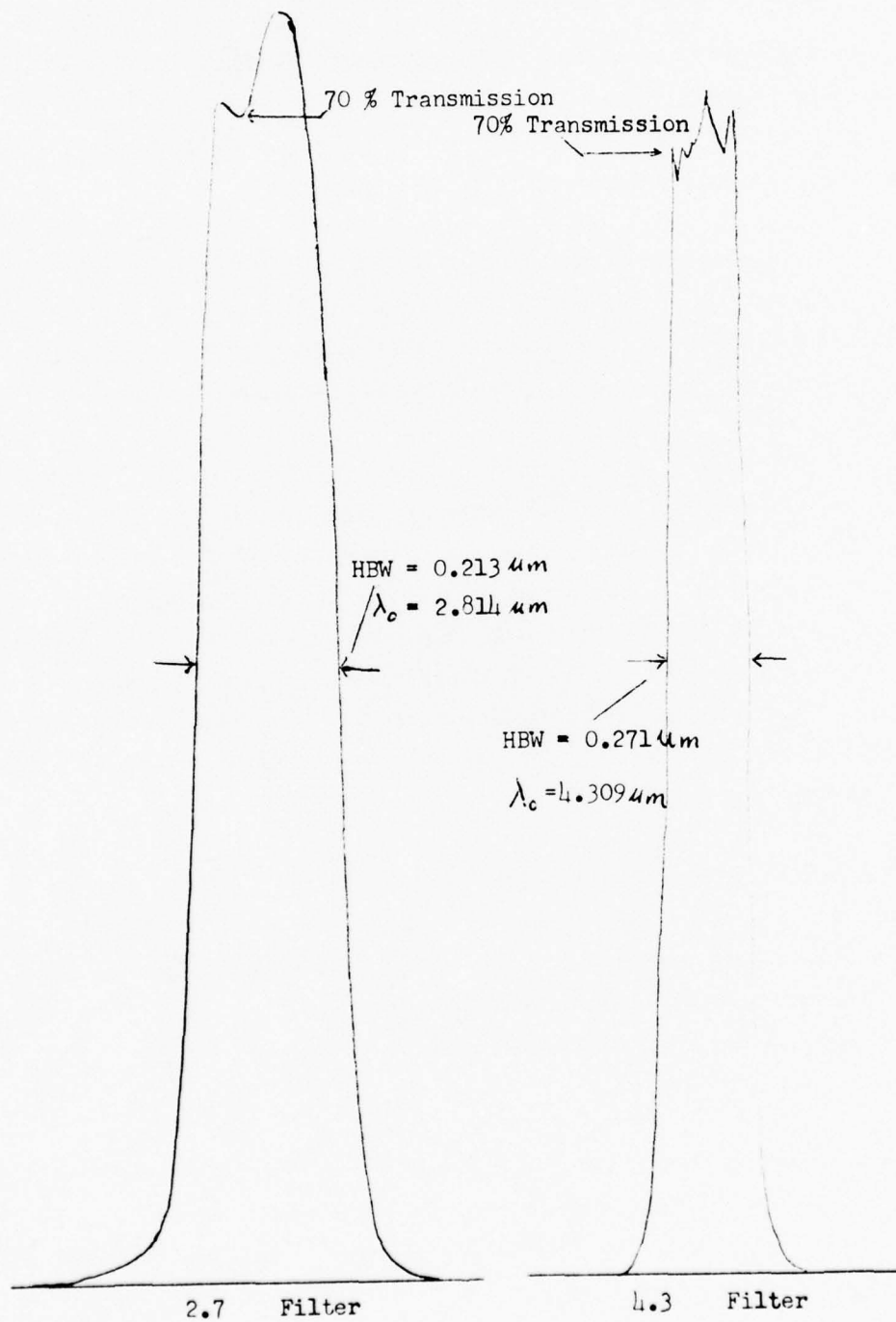


Figure 2 Filter Spectra

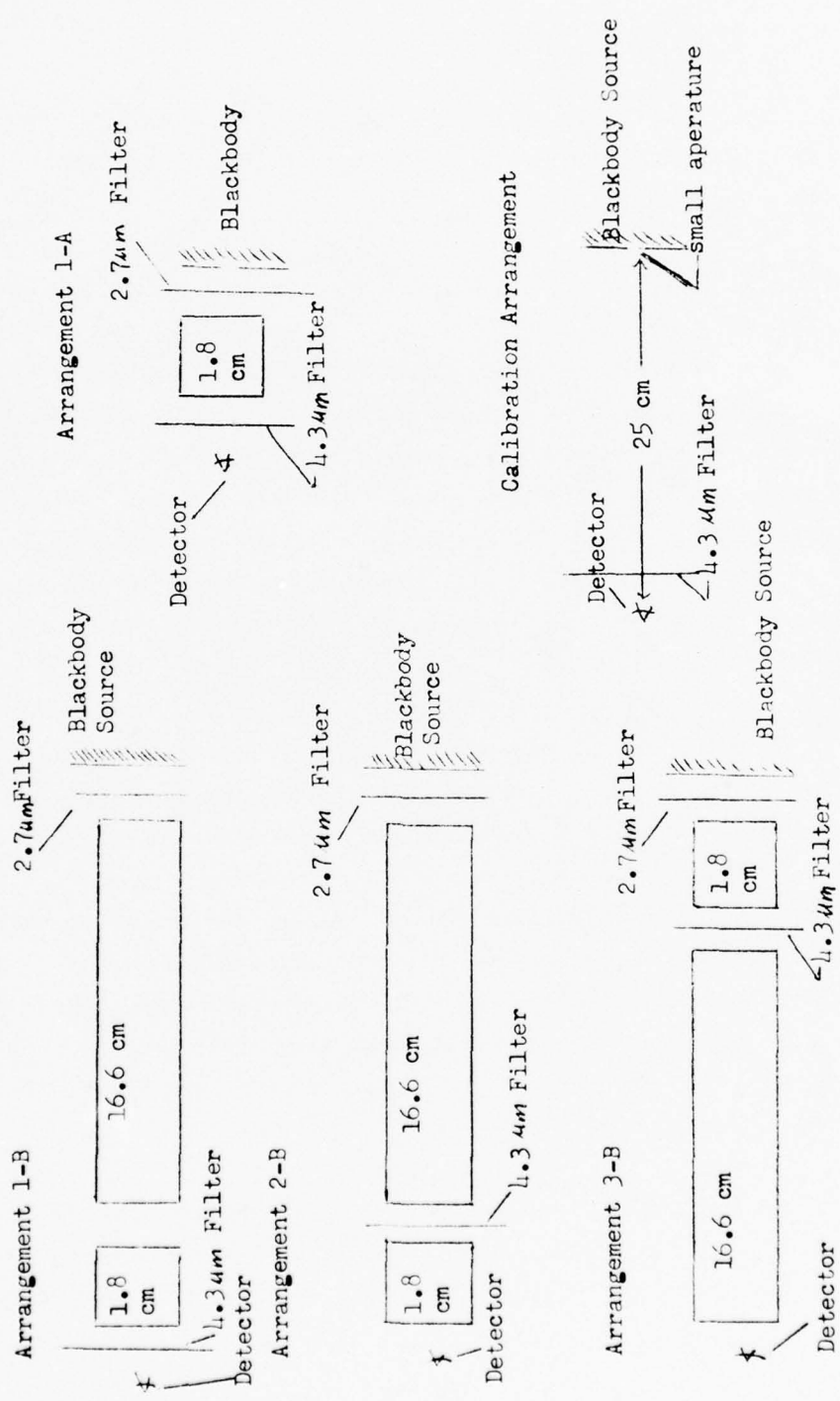


Figure 3 Summary of Experimental Arrangements Used in This Study

Addition of 60 Torr of Ne to the fluorescence cell containing 7.5 Torr of  $\text{CO}_2$  resulted in an increase of signal to  $9.8 \times 10^{-12}$  watts.

Additional measurements utilizing arrangement 2-B were made. The resulting change inserting or removing the filter cell were the same, namely essentially no effect on signal.

For convenience we summarize a number of these results, plus the ones already mentioned, in table (1). We also show the calculated transmission through the filter cell which is expected for the 021-020 band and the 001-000 band. The band transmission functions were calculated as discussed in, section (II). We show the results for values of the parameter  $a$  describing a voigt profile of  $a = 0$ ,  $a = 1$  and  $a = 1.5$ . (Recall that  $a = 0$  corresponds to a Doppler lineshape.) We have only included measurements where the pressures in the fluorescence cell and filter cell are similar or the band transmission functions are calculated assuming identical line shapes for the absorbing and emitting lines.

Inspection of this table shows that essentially none of the signal is absorbed by the  $\text{CO}_2$  filter cell. The calculated transmission of the fluorescent bands is of the order of 90% since the pressures used correspond to an  $a$  value of 1.5. The fact that the transmission for the resonance 001-000 band is less than 5% suggests that the observed signal cannot be due to the resonance band. The results are more nearly what one would expect for the fluorescent band 021-020. Even here the transmission is greater than the calculated value. This could be due to the fact that the lines may be more broadened by Ne than suggested by our choice of  $0.05 \text{ cm}^{-1} \text{ ATm}$  for the Ne pressure broadening coefficient.

In view of the results using arrangement 2-B we decided to interchange the filter cell and the fluorescence cell so as to increase the amount of absorption obtainable with the filter cell. This resulted in arrangement 3-B of figure (3).

TABLE I Attenuation of 4.3  $\mu\text{m}$  Radiation by  $\text{CO}_2$  using arrangement 2-B of figure 3.

16.6 cm Cell	1.8 cm Cell	Signal With No Filter	$N\sigma$ of Filter Cell	Calc. Transmission	Observed Transmission	
			021-020 Band	021-020 Band	001-000 Band	
1 Torr $\text{CO}_2$ + 60 Torr Ne	8 Torr $\text{CO}_2$ + 60 Torr Ne	$1.19 \times 10^{-11}$ w	19.4	$T_0 = 70\%$ $T_1 = 88\%$ $T_{1.5} = 92\%$	$T_0 < T_1$ $T_1 < T_{1.5}$ $T_{1.5} = 5\%$	100%
7.5 Torr $\text{CO}_2$ + 60 Torr Ne	Same As Above	$9.8 \times 10^{-11}$ w				
2 Torr $\text{CO}_2$ + 50 Torr Ne	9 Torr $\text{CO}_2$ + 51 Torr Ne	$1.7 \times 10^{-11}$ w	21.8	$T_0 = 68\%$ $T_1 = 87\%$ $T_{1.5} = 88\%$	$T_0 < T_1$ $T_1 < T_{1.5}$ $T_{1.5} = 4.8\%$	100%

Due to the experimental procedure, the observed transmission is uncertain by a few percent. In this arrangement the 16.6 cm cell is the fluorescence cell.

In Table 2 we summarize two sets of measurements which were made with this configuration.

The results of Table 2 are similar to those in Table 1 in that they also suggest that the radiation observed is due to the fluorescent bands rather than due to the resonance band.

The quantitative agreement between observed and calculated transmissions is not completely satisfactory. In the case of pure  $\text{CO}_2$  in both cells at 2 mm pressure, the pressure broadened linewidth should be only about 4% of the Doppler width based on our discussion of Section (II). Therefore, we expect that the transmission would be less than .76 calculated for  $a = 1$ , and only slightly greater than the value .48 calculated for pure Doppler line shape. The transmission appears to be greater than we expect.

Additional experiments will be required before a detailed evaluation of this data is possible. Also, it seems likely that it may be necessary to allow for the variation of linewidths with rotational state in accurate calculations of the transmission functions.

Certainly the qualitative conclusion to be inferred from the comparisons given above strongly suggest that the observed 4.3  $\mu\text{m}$  signal is due to fluorescence rather than resonance radiation. This conclusion is in distinct contradiction to the value of  $1.3 \times 10^{-10}$  for the rate constant of reactions 2 which would indicate that at 2 mm pressure the rate of loss of (O21)  $\text{CO}_2$  molecules would be

$$k = (1.3 \times 10^{-10}) \quad n = 6.52 \times 10^{16}/\text{cc}$$

$$\text{Rate} = 8.5 \times 10^6 \text{ sec}^{-1}$$

which is greater than the radiative rate of  $420 \text{ sec}^{-1}$  by a factor of  $2 \times 10^4$ . Calculations described in the following section treating the magnitude of the observed signals suggest that the quenching of the observed signal is much slower than expected for  $k = 1.3 \times 10^{-10}$ .

TABLE II Attenuation of 4.3  $\mu$ m Radiation by CO<sub>2</sub> using arrangement 3-B of figure 3.

1.8 cm Cell	16.6 cm Cell	Signal With No Filter	N of Filter Cell	Calc. Transmission		Observed Transmission
				021-020 Band	001-000 Band	
2 Torr CO <sub>2</sub>	2 Torr CO <sub>2</sub>	1.26 10 <sup>-11</sup> w	44.6	$T_0 = 48\%$ $T_1 = 76\%$ $T_{1.5} = 82\%$	$T_0 = 9 \times 10^{-4}$ $T_1 = 3.3 \times 10^{-2}$	70%
2 Torr CO <sub>2</sub>	1 Torr CO <sub>2</sub> + 60 Torr Ne	1.39 10 <sup>-11</sup> w	22.3	$T_0 = 67\%$ $T_1 = 86\%$ $T_{1.5} = 90\%$	$T_0 < T_1$ $T_1 < T_{1.5}$ $T_{1.5} = 6\%$	61%

Due to the experimental procedure, the observed transmission is uncertain by a few percent. In this arrangement the 1.8 cm Cell is the fluorescence cell. The subscript on the calculated transmission refers to the parameter a characterizing a Voigt Profile. a=0 is the pure Doppler case.

Our results at the present time seem to indicate that the observed signal is due to fluorescence and that the rate constant for reaction 2 must be much greater than  $1.3 \times 10^{-10}$  by several orders of magnitude.

Another possibility which we should consider is that the rate constant for reactions 2(a) is actually  $1.3 \times 10^{-10}$ . With such a rapid rate, we might expect rapid equilibration of the  $\nu_3$  vibration between all levels of  $\text{CO}_2$  which are thermally populated and between all isotopic molecules. Due to the fact that many lines of the 001-000 band are optically thick under the conditions of this experiment, it is possible that the observed signal has a large contribution from weak bands which are either hot bands or isotope bands. In order to explore this possibility we present in table 3, the results of a calculation which includes the more important isotope bands and hot bands.

In making the calculation shown in table (3), we have assumed that the excitation in the 021-000 and 101-000 bands at 2.77 and 2.69  $\mu\text{m}$  is essentially constant throughout the 1.8 cm fluorescence cell. In this case a reasonable approximation to the emission from this cell will be given by the width functions for the bands at 4.3  $\mu\text{m}$ .

The  $N\sigma$  values for the bands listed in table 3 are calculated assuming a Boltzman distribution of all of the levels involved and using normal isotopic abundances. The signal observed will be proportional to the product of  $W_b(N\sigma)$  in the fluorescence cell and the transmission of that band through the filter cell  $T_b(N\sigma)_{\text{Filter}}$ . The transmission calculated for all bands together is just the ratio of the signal with the filter in place to the value with the filter removed and is given by

$$T = \frac{\sum_k W_k(N\sigma)_{\text{Fluorescent}} \cdot T_b(N\sigma)_{\text{Filter}}}{\sum_k W_k(N\sigma)_{\text{Fluorescent}}}$$

where the sum  $k$  is over all the lines in the band. In this case the calculated transmission of .05 is still well below the observed value of approximately 70%.

TABLE III Calculated Relative Signal and Transmission Assuming a Boltzman Distribution for the Lower Level of the Bands Shown and Assuming a Doppler Line Shape.

Band	$N\sigma$ For 1.8 cm Cell	$W(N\sigma)$ For Fluorescence Cell	$N\sigma$ For Filter Cell	Filter Cell Transmission	Product $W(N\sigma) \cdot T$
<b>626 Isotope</b>					
001-000	$2.55 \cdot 10^3$	120	$2.35 \cdot 10^4$	$9.1 \cdot 10^{-4}$	0.11
021-020	4.84	4.84	44.6	0.48	2.32
101-100	2.93	2.93	27	0.62	1.82
011-010	$1.97 \cdot 10^2$	67.3	$1.82 \cdot 10^3$	$1.6 \cdot 10^{-2}$	1.07
<b>636 Isotope</b>					
001-000	27.9	7.96	259	$9.4 \cdot 10^{-2}$	.75
011-010	2.17	2.17	20	0.69	1.5
<b>628 Isotope</b>					
001-000	10.2	9.1	95.4	.26	2.37
011-010	0.79	0.79	7.38	.83	0.66
<b>627 Isotope</b>					
001-000	1.85	1.85	17.2	.73	1.35



These calculations are not quantitatively exact. The width function for the 021-000 band in the fluorescence cell is  $W_b(N\sigma) = 18.5$  whereas the value of  $N\sigma$  is 22.75 which indicates that the excitation is not strictly uniform along the length of the 1.8 cm cell. The variation is not drastic, however and the results presented in table 3 should remain qualitatively unchanged. That is, even considering many weak bands does not explain the high observed transmission. It seems as though the only reasonable explanation for this high transmission is that the observed signal is predominately due to the fluorescent bands 021-020 and 101-100.

VI. Determination of Approximate Quenching Rates From Absolute Intensity Measurements

Measurements of the absolute radiance at 4.3  $\mu\text{m}$  produced by irradiating  $\text{CO}_2$  at 2.7  $\mu\text{m}$  were made using the arrangement shown in figure (3) arrangement 1-A. With this arrangement the signals are larger than with the other arrangements and the geometry lends itself to simpler calculations. We use the following expression for the observed signal

$$\text{Signal (watts)} = \frac{W}{\pi} \left( \frac{W}{\pi} \right)_{2.7} \Omega_s A_s \frac{A_D}{4\pi} \frac{x_2}{(l-x_2)l} S_b \frac{2.7}{4.3} \frac{W(N\sigma)}{(N\sigma)_{4.3}} T_{4.3}^R$$

The blackbody temperature was 1148.4  $^\circ\text{K}$ . The resulting blackbody radiances are:

$$\left( \frac{W}{\pi} \right)_{2.76\mu\text{m}} = 0.797 \text{ w/cm}^2 \text{ - } \mu\text{m-Sr}$$

$$\left( \frac{W}{\pi} \right)_{2.69 \mu\text{m}} = 0.809 \text{ w/cm}^2 \text{ -}\mu\text{m-Sr.}$$

The transmission of the filter at 2.76  $\mu\text{m}$  is 73% and at 2.68  $\mu\text{m}$  is 18%. This filter is shown in fig. 2. If  $S_b(\lambda)$  represents the band strength per cm of path under the conditions of the experiment, then total rate of excitation per cm of path in the fluorescence cell is

$$\text{Total watts absorbed} = [(.797)(.73)S_b(2.76) + (.809)(.18)S_b(2.69)] \Omega_s A_s$$

Where  $\Omega_s$  is the solid angle which the front face of the fluorescence cell makes with a point at the source and  $A_s$  is the area of the source.

Figure 4 shows the geometry used in this calculation.  $A_s$  is taken as the area of the blackbody cavity opening which is 3.24  $\text{cm}^2$ .  $\Omega_s$  is taken as the area of the 2.7  $\mu\text{m}$  filter divided by the square of the distance to the blackbody opening which is 3.8 cm. This gives an effective solid angle of .22 Sr. For points near the edge of the blackbody, the 2.7  $\mu\text{m}$  filter subtends a smaller solid angle, therefore, we choose 0.2 Sr as an approximate value

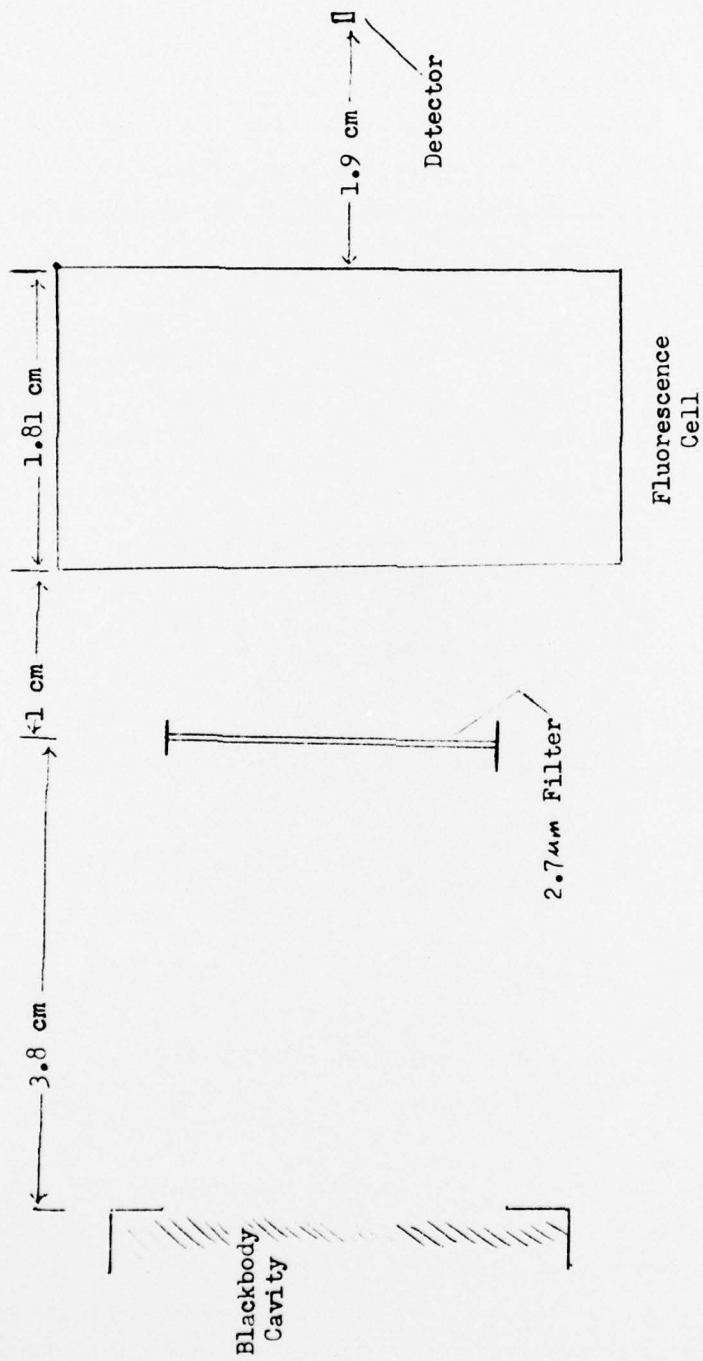


Figure 4 Geometrical Arrangement for Absolute Intensity Measurement.

for  $\Omega_s$ . The signal in watts has a factor  $\frac{2.7}{4.3}$  since for a given number of photons, the number of watts is smaller at 4.3 than at 2.7 by this ratio.  $x_2$  is seen from figure 4 to be 1.9 cm and  $l$  is 3.7 cm. The detector has an area of 0.0314 cm<sup>2</sup>.  $T_{4.3}$  is the transmission of the 4.3  $\mu$ m filter placed in front of the detector. This has a transmission of 70% and is shown in fig (2).

If the band strengths are expressed in wave numbers, then it is convenient to multiply the blackbody radiances by  $7.3 \times 10^{-4}$  to convert from watts/ $\mu$ m-Sr-cm<sup>2</sup> to watts/cm<sup>-1</sup>-Sr-cm<sup>2</sup>.

The total signal expected is:

$$\begin{aligned}
 & (.797)(.73)S_b(2.76) \left[ 1 + \left( \frac{.809}{.797} \right) \left( \frac{.18}{.73} \right) \left( \frac{S_b(2.69)}{S_b(2.76)} \right) \right] \\
 & \times 7.3 \times 10^{-4} (.2)(3.24)(.0314) \left( \frac{1}{4\pi} \right) (.7) \left( \frac{2.7}{4.3} \right) \\
 & \times \frac{W(N\sigma)}{(N\sigma)_{4.3}} \cdot \frac{x_2}{(l-x_2)(l)} \cdot R \\
 & = [1.34](3.02 \times 10^{-7})S_b(2.76) \cdot \frac{W(N\sigma)}{(N\sigma)_{4.3}} \cdot \frac{x_2}{(l-x_2)l} \cdot R
 \end{aligned}$$

This result is expressed in terms of the absorption occurring for the 2.76  $\mu$ m band times a factor 1.34 to account for the fact that under the conditions of our experiment the 101-000 band is contributing about .34 times the contribution of the 021-000 band to the total excitation rate. We consider a measurement where the total pressure of CO<sub>2</sub> 7 mm Hg with no added gas.

The band strength under these conditions is

$$\begin{aligned}
 S_b & = \frac{37.4(\text{cm}^{-1}/\text{ATm-cm})}{760 \text{ Torr}/\text{ATm}} \cdot \left( \frac{273}{290} \right) \times 7 \text{ Torr} \\
 & = 0.317 \text{ cm}^{-1}/\text{cm}
 \end{aligned}$$

The factor  $x_2/(l-x_2)l = 0.28$ . Combining these factors gives:

$$\text{Signal} = 3.59 \times 10^{-8} \left[ \frac{W(N_0)}{(N_0)_{4.3}} \right] \cdot R$$

In this expression  $R$  is the ratio of  $4.3 \mu\text{m}$  photons emitted to the quenching of levels emitting at  $4.3 \mu\text{m}$ . The ratio  $(W/N_0)$  is included to account for the fact if the  $4.3 \mu\text{m}$  emission is occurring in optically thick bands, then the radiation escaping will be reduced by this factor due to self absorption. If we assume that the emitted radiation occurs in the bands 021-020 and 101-100, the  $N_0$  values for these bands are 16.94 and 10.24 with corresponding values of  $W(N_0)/N_0$  of .86 and .91 respectively for Doppler line shape and .94 and .96 for Voigt profiles with  $a = 1$ . Since the Lorentz Pressure broadened width is almost as large as the Doppler width, the  $a = 1$  value is a better choice. We therefore, take  $W(N_0)/N_0$  to be  $\sim .94$ . This gives a calculated signal of:

$$\text{Signal} = 3.37 \times 10^{-8} \text{ watts.}$$

The observed signal has a value of  $2 \times 10^{-2} \text{ mv} \div 2.14 \times 10^8 \text{ mv/watt} = 9.34 \times 10^{-11}$  watts. This implies that  $R$  has a value of  $2.77 \times 10^{-3}$ .

$$R \text{ can be expressed as } R = \frac{A}{A + Q}$$

where  $A = 420 \text{ sec}^{-1}$  is the  $4.3 \mu\text{m}$  Einstein emission rate and  $Q$  is the quenching rate. At 7 Torr  $Q$  has a value

$$Q = (3.26 \times 10^{16})(7)(k)$$

where  $k$  is the quenching rate constant.

From the above value of  $R$ , the quenching rate constant is

$$k = 6.6 \times 10^{-13} \text{ cm}^3 \text{ sec}^{-1}$$

While these calculations are not highly accurate quantitatively, they do indicate that if the observed radiation is truly fluorescence then the quenching

of these levels is not occurring nearly as rapidly as would be suggested with a value of  $1.3 \times 10^{-10}$  for reactions 2(a).

If, for comparison, we assume that the radiation at  $4.3 \mu\text{m}$  is occurring in the resonance band 001-000, then the value of  $N_0$  for the  $4.3 \mu\text{m}$  bands is  $8.91 \times 10^3$  and the corresponding ratio  $W(N_0)/N_0$  is  $\sim .105$ . With this value of  $W(N_0)/N_0$ , the resulting value of  $R$  is

$$R \approx 2.48 \times 10^{-2}$$

With this value of  $R$ , and the same rate constant expression as given above, the quenching rate constant becomes:

$$k \sim 7.24 \times 10^{-14}$$

These estimates of  $k$  cannot be considered to be accurate because the geometry is such that our simple calculation is not adequate. Furthermore, the calculations assume that the rate of absorption in the  $2.7 \mu\text{m}$  bands is uniform along the  $1.8 \mu\text{m}$  length of the fluorescence cell. Consider the  $2.76 \mu\text{m}$  band for which the  $N_0$  value at  $1.8 \text{ cm}$  path and  $7 \text{ Torr}$  is  $79$ . For this value of  $N_0$ , the bandwidth function  $W(N_0)$  has a value of  $63$  which would decrease the calculated signal by about  $21\%$ .

Thus in the case of the assumption of purely fluorescent bands the value of  $k$  obtained should be reduced about  $21\%$  to yield

$$k \sim 5.2 \times 10^{-13}$$

In the case of the assumption of purely resonance bands, the value of  $k$  should be reduced even more since due to the large optical depth of the resonance band only radiation originating very close to the exit window can escape.

In this case it is really necessary to consider the excitation occurring at a given point along the fluorescence cell and calculating the fraction of  $4.3 \mu\text{m}$  radiation emitted from that point which can reach the exit window of

the cell. This requires an integration of the product of the volume emission rate and the transmission.

The total  $N_0$  of 79 for the 2.76  $\mu\text{m}$  band results in a width function of 63. If we consider the amount of absorption occurring in the last 10% of the path length for a total  $N_0$  of 71. + 7.9 the contribution to  $W(N_0)$  from the first 90% of path is approximately 58 as compared with 5 for the last 10%. Therefore, the amount of 2.7  $\mu\text{m}$  radiation being absorbed next to the exit window per unit volume is occurring at a rate which is 5/7.9 or about 63% less than the rate of absorption calculated for optically thin 2.7  $\mu\text{m}$  bands. The optical depth of this last 1/10 of path length for the 4.3 bands if they are assumed to be resonance bands is  $N_0 = 8.91 \times 10^2$  for which  $W(N_0) \approx 2.90 \times 10^2$ . Therefore  $W(N_0)/(N_0) \approx .325$ . The signal from this portion is down from the purely non-optically thick case by

$$(.1) \left( \frac{5}{7.9} \right) (.325)$$

The other 90% of molecules contribute

$$\left( \frac{58}{79} \right) \times \left( \frac{W(8.93 \times 10^3 \times .9)}{(8.93 \times 10^3 \times .9)} \right)$$

The transmission of this radiation through the remaining 10% of path length is  $\sim .175$ . Combining these factors yields a loss of signal of the order of .034 rather than .105, which suggests that

$$R \text{ should be approximately } 7.65 \times 10^{-2}$$

which yields  $k = 2.2 \times 10^{-14}$ .

While more exact calculations should be carried out, we have uncertainties and variations from several different experiments of the order of 15 to 20% so that until our experimental technique is refined, these approximate calculations are sufficient for a qualitative assessment of our results.

Experiments with the same arrangement discussed in the above experiment have been treated in a similar manner and yield similar results. In the case of pure CO<sub>2</sub> at 1.5 Torr, the treatment described above yields an observed signal of  $8.83 \times 10^{-11}$  watts and the following results.

$$k \sim 7.4 \times 10^{-13} \text{ cm}^3 \text{ sec}^{-1} \text{ if radiation assumed to be fluorescence}$$

and  $k \sim 3.8 \times 10^{-14} \text{ cm}^3 \text{ sec}^{-1}$  if radiation assumed to be 001-000 resonance radiation.

When the pressure was reduced to 280 Torr of pure CO<sub>2</sub>, a signal of about  $3.08 \times 10^{-11}$  was observed. In this case the values obtained for  $k$  were larger, being

$$k \sim 2 \times 10^{-12} \text{ if the signal is assumed to be fluorescence}$$

and

$$k \sim 1.4 \times 10^{-12} \text{ if it is assumed to be resonance.}$$

At these low pressures in pure CO<sub>2</sub>, the apparent increase in the quenching rate is probably due to loss of excited molecules in collisions with the walls. Certainly the results at 280 micron Hg are unreliable due to quenching by wall collisions. At pressures above a few mm Hg, diffusion to the walls should not be an important loss mechanism.

While our experiments at this stage do not permit us to draw quantitative conclusions, we can make some qualitative statements. If we assume that the observed radiation at 4.3  $\mu\text{m}$  is predominately due to the 001-000 band, then we obtain values of the quenching rate constant of the order of  $2 \times 10^{-14}$ . This is not an unreasonable value, since accepted rate constant for the quenching of the 001 level have been reported to be of this order of magnitude. This interpretation does not agree with our experiments using CO<sub>2</sub> as a filter which suggests that most of the radiation is in the bands 021-020 and 101-100.

In order that most of the radiation be in bands 101-100 and 021-020, the rate constant of reaction 2(a) cannot be as large as  $1.3 \times 10^{-10}$ . The fact



that the transmission experiments suggest that very little of the radiation observed is in the band 001-000 and the fact that the intensity measurements, based on the assumption of fluorescent bands being the major contributor, leads to a quenching rate constant of the order of  $5 \times 10^{-13}$  both tend to support the interpretation of the  $4.3 \mu\text{m}$  radiation as arising from fluorescent bands.

## VII. SUMMARY AND DISCUSSION OF RESULTS

We have conducted experiments in which it has definitely been established that  $4.3 \mu\text{m}$  radiation is produced when  $\text{CO}_2$  is irradiated with  $2.7 \mu\text{m}$  radiation. Our summary of attenuation measurements in section V and the summary of absolute intensity measurements in section VI suggest that a large portion of the observed radiation arises from bands 021-020 and 101-100 rather than from the 001-000 band.

In examining our attenuation calculations we should point out the fact that the transmission through the filter cell is calculated assuming that the lineshapes of the radiation emerging from the fluorescence cell are the same as for the absorption cell. Since the emerging radiation will be from optically thick samples if it is due to the resonance band 001-000, there should be considerable radiation in the wings of the lines, so that our calculated transmission for the 001-000 band is not really correct, and the actual transmission will be higher than that calculated in tables I, II, and III for the optically thick bands. What is required is an integration of the volume emission rate times the transmission through the gas between the emitting region and the detector. This will include a transmission through both the fluorescence cell and the filter cell. A comparison of these results with and without the filter cell in place would correspond to our experimental measurement. If the total  $N\sigma$  of the fluorescence cell is  $N\sigma_1$  and the total  $N\sigma$  of the filter cell is  $N\sigma_2$  and it is assumed that all of the excitation occurs near the front face of the fluorescence cell (i.e., the window farthest away from the filter cell) then the signal without the filter cell in place would be proportional to  $T(N\sigma)_1$  and with the filter cell in place it would be proportional to  $T(N\sigma_1 + N\sigma_2)$ . This places an upper limit on the observed transmission of

$$(T_{\text{obs}})_{\text{max}} = \frac{T(N\sigma_1 + N\sigma_2)}{T(N\sigma_1)}$$

Considering the arrangement in Table II where for the fluorescence cell  $N\sigma_1$  is  $2.55 \times 10^3$  and  $N\sigma_2$  is  $2.349 \times 10^4$  for the first entry, the values of  $N\sigma$ 's result in

$$\begin{aligned}
 (T_{\text{obs}})_{\text{max}} &= 9.8 \times 10^{-2} \text{ for } a = 0 \\
 &= .31 \text{ for } a = 1
 \end{aligned}$$

These numbers are considerably higher than the values shown in the table. Since the excitation is essentially uniform along the fluorescence cell, the actual transmission should be smaller than these figures suggest. The fact that our observed transmission is still greater than these upper limits suggests that much of the observed signal can still be regarded as fluorescence rather than resonance radiation. A calculation for all the bands of Table III in which we calculate the ratio

$$\frac{\sum (N\sigma_1) T (N\sigma_1 + N\sigma_2)}{\sum (N\sigma_1) T (N\sigma_1)}$$

and use this result in table III rather than just the filter cell transmission shows that an upper limit to the transmission as calculated using all of the bands in table III is approximately 20% rather than the calculated 5% shown below table III.

While our results may be misleading as shown in tables I, II, and III, we still feel that there is evidence for an appreciable contribution from the fluorescent bands rather than the resonance bands. At the present stage of these experiments it is probably premature to make any definite statements regarding the composition of the observed 4.3  $\mu\text{m}$  radiation. Until such time as detailed radiative transport calculations are carried out under a variety of carefully selected experimental arrangements, we cannot arrive at definitive values for the composition of the 4.3  $\mu\text{m}$  radiation.

Our estimates of the amount of quenching taking place cannot be considered reliable until such a detailed radiative transport calculation is carried out. It is probably preferable to determine quenching rates from detailed measurements of the pressure dependence of the emission rather than from absolute intensity measurements. Such measurements are far from simple, however, in that

changing the pressures of  $\text{CO}_2$  and/or added gases not only changes the quenching rates, but also changes the line shapes and therefore affects the calculation of the radiative transport functions required in reducing the data. Utilizing carefully selected experimental conditions should lead to a complete understanding of the mechanisms determining the composition and intensity of the fluorescence.

We expect to examine the possibility that laser excitation might lead to results which differ from those obtained utilizing a continuous source. Since rotational redistribution is expected to take place rapidly at very low pressures, it seems unlikely that the two excitation methods would require different treatments. We are considering the use of a  $10.6 \mu\text{m}$  laser to excite the 001 level and then examine the resultant  $4.3 \mu\text{m}$  emission. Measurements of the transmission characteristics of this radiation under a variety of conditions may aid in understanding the high transmissions observed in our experiments.

In the event that our results can only be explained on the basis of a value of  $k$  for reaction (2) which is orders of magnitude smaller than  $1.3 \times 10^{-10}$ , then it will be necessary to find an alternative explanation for the laser studies which produced this result. Until such time as we have completely explained our results, it is probably not advisable to seek an alternative explanation.

It is clear that a detailed understanding of this laboratory experiment will involve a theoretical treatment which will be applicable to several important applications involving the transport of radiation in the atmosphere. The laboratory studies will provide a method for verifying such theoretical treatments of atmospheric radiative transfer problems and ultimately increase the credibility of the theory.

References

- (1) T. C. James, J. B. Kumer, "Fluorescence of CO<sub>2</sub> Near 4.3 μm. Application to Daytime Limb Radiance Calculations." J. Geophys. Res. 78, 8320(1973)
- (2) Nickerson, "Equilibrium Radiation Model for Exhaust Plumes." AFRPL-TR-74-74, March 1975
- (3) J. Finzi and C. B. Moore, "Relaxation of CO<sub>2</sub> (101), CO<sub>2</sub> (021), and N<sub>2</sub>O (101) vibrational levels by near-resonant V → V energy energy transfer. J. Chem. Phys. 63, 2285 (1975)
- (4) J. B. Kumer and T. C. James, "CO<sub>2</sub>(001) and N<sub>2</sub> Vibrational Temperatures in the 50 ≤ z ≤ 130 km Altitude Range. J. Geophys. Res. 79, 638 (1974)
- (5) Kaplan and Eggers, J. Chem. Phys. 25, 876 (1956)

## DISTRIBUTION LIST

### DEPARTMENT OF DEFENSE

Director  
Defense Advanced Research Proj. Agency  
ATTN: LTC W. A. Whitaker  
ATTN: Major Gregory Canavan  
ATTN: STO, Captain J. Justice

Defense Documentation Center  
12 cy ATTN: TC

Director  
Defense Nuclear Agency  
ATTN: STSI, Archives  
ATTN: RAAE, Major John Clark  
3 cy ATTN: RAAE, Charles A. Blank  
ATTN: RAEV, Harold C. Fitz, Jr.  
3 cy ATTN: STTL, Tech. Library

Dir. of Defense Research & Engineering  
Department of Defense  
ATTN: S&SS (OS)

Commander  
Field Command  
Defense Nuclear Agency  
ATTN: FCPR

Chief  
Livermore Division, Field Command, DNA  
Lawrence Livermore Laboratory  
ATTN: FCPRL

### DEPARTMENT OF THE ARMY

Commander/Director  
Atmospheric Sciences Laboratory  
US Army Electronics Command  
ATTN: DRSEL-BL-SY-S, F. E. Niles

Commander  
Harry Diamond Laboratories  
2 cy ATTN: DRXDO-NP

Commander  
US Army Nuclear Agency  
ATTN: MONA-WE

Commander  
US Army Foreign Science & Tech. Center  
ATTN: R. Jones

### DEPARTMENT OF THE NAVY

Chief of Naval Research  
Navy Department  
ATTN: Code 464

Commander  
Naval Ocean Systems Center  
ATTN: Code 2200, Verne E. Hildebrand  
ATTN: Code 2200, Ilan Rothmuller

### DEPARTMENT OF THE NAVY (Continued)

Director  
Naval Research Laboratory  
ATTN: Code 7127, Charles Y. Johnson  
ATTN: Code 7750, Paul Julienne  
ATTN: Code 7701, Jack D. Brown  
ATTN: Code 7750, Darrell F. Strobel  
ATTN: Code 7750, Wahab Ali  
ATTN: Code 2600, Tech. Lib.  
ATTN: Douglas P. McNutt  
ATTN: Code 7700, Timothy P. Coffey

Commander  
Naval Surface Weapons Center  
ATTN: Code WA501, Navy Nuc. Prgms. Off.

### DEPARTMENT OF THE AIR FORCE

AF Geophysics Laboratory, AFSC  
5 cy ATTN: LKB, Kenneth S. W. Champion  
ATTN: OP, John S. Garing  
ATTN: OPR, Alva T. Stair  
5 cy ATTN: OPR, J. Ulwich  
ATTN: LKD, R. Narcisi

AF Weapons Laboratory, AFSC  
ATTN: SUL  
ATTN: DYT, Lt Col Don Mitchell

Commander  
ASD  
ATTN: ASD-YH-EX, Lt Col Robert Leverette

SAMSO/SZ  
ATTN: SZJ, Major Lawrence Doan

### ENERGY RESEARCH & DEVELOPMENT ADMINISTRATION

Division of Military Application  
US Energy Research & Dev. Admin.  
ATTN: Doc. Con. for Major D. A. Haycock

Los Alamos Scientific Laboratory  
ATTN: Doc. Con. for R. A. Jeffries

### OTHER GOVERNMENT AGENCIES

Department of Commerce  
Office of Telecommunications  
Institute for Telecom Science  
ATTN: William F. Utlaut

### DEPARTMENT OF DEFENSE CONTRACTORS

Aerodyne Research, Inc.  
ATTN: F. Bien  
ATTN: M. Camac

Aerospace Corporation  
ATTN: R. Grove  
ATTN: R. D. Rawcliffe  
ATTN: Harris Mayer  
ATTN: Thomas D. Taylor  
3 cy ATTN: R. J. McNeil

DEPARTMENT OF DEFENSE CONTRACTORS (Continued)

University of Denver  
Colorado Seminary  
Denver Research Institute  
ATTN: Sec. Officer for David Murcraay  
ATTN: Sec. Officer for Mr. Van Zyl

General Electric Company  
TEMPO-Center for Advanced Studies  
5 cy ATTN: DASIAC, Art Feryok  
ATTN: Warren S. Knapp

General Research Corporation  
ATTN: John Ise, Jr.

Geophysical Institute  
University of Alaska  
3 cy ATTN: Neal Brown  
ATTN: T. N. Davis

Honeywell Incorporated  
Radiation Center  
ATTN: W. Williamson

Institute for Defense Analyses  
ATTN: Hans Wolfhard  
ATTN: Ernest Bauer

Lockheed Missiles & Space Company, Inc.  
ATTN: John B. Cladis, Dept. 52-12  
ATTN: Tom James  
ATTN: J. B. Reagan, D/52-12  
ATTN: John Kumer  
ATTN: Richard G. Johnson, Dept. 52-12  
ATTN: Martin Walt, Dept. 52-10  
ATTN: Robert D. Sears, Dept. 52-14  
ATTN: Billy M. McCormac, Dept. 52-54

Mission Research Corporation  
ATTN: D. Archer  
ATTN: P. Fischer  
ATTN: P. Sappenfield

Photometrics, Inc.  
ATTN: Irving L. Kofsky

Physical Dynamics, Inc.  
ATTN: Joseph B. Workman

DEPARTMENT OF DEFENSE CONTRACTORS (Continued)

Physical Sciences, Inc.  
ATTN: Kurt Wray

R & D Associates  
ATTN: Robert E. LeLevier  
ATTN: Forrest Gilmore

R & D Associates  
ATTN: Herbert J. Mitchell

The Rand Corporation  
ATTN: James Oakley

Science Applications, Inc.  
ATTN: Daniel A. Hamlin

Space Data Corporation  
ATTN: Edward F. Allen

Stanford Research Institute  
ATTN: Ray L. Leadabrand  
ATTN: M. Baron  
ATTN: Walter G. Chestnut

Stanford Research Institute  
ATTN: Warren W. Berning

Technology International Corporation  
ATTN: W. P. Boquist

Utah State University  
ATTN: D. Burt  
ATTN: C. Wyatt  
ATTN: Kay Baker  
ATTN: Doran Baker

VisiDyne, Inc.  
ATTN: Charles Rumphrey  
ATTN: J. W. Carpenter  
ATTN: L. Katz  
ATTN: Henry J. Smith  
ATTN: William Reidy  
ATTN: T. C. Degges